9 Magnetic Resonance Spectroscopy Methods

Eduardo Coello, Tyler C. Starr, and Alexander P. Lin

Contents

E. Coello · T. C. Starr · A. P. Lin (✉)
Department of Radiology, Center for Clinical Spectroscopy, Brigham and Women's Hospital, Harvard Medical School, Boston, MA, USA
e-mail: jcoellouribe@bwh.harvard.edu; tstarr@bwh.harvard.edu; aplin@bwh.harvard.edu

M. Kubicki, M. E. Shenton (eds.), *Neuroimaging in Schizophrenia*,
https://doi.org/10.1007/978-3-030-35206-6_9

Abbreviations

13C	Carbon 13
2D COSY	Two-Dimensional COrrelated SpectroscopY
2D JPRESS	Two-Dimensional J-resolved Point RESolved Spectroscopy
Cho	Choline
Cr	Creatine
CRLB	Cramer–Rao lower bounds
CSI	Chemical shift imaging
FT	Fourier transform
FID	Free induction decay
fMRI	functional magnetic resonance imaging
GABA	*gamma*-Aminobutyric acid
Gln	Glutamine
Glu	Glutamate
Glx	Both glutamate and glutamine
GPC	Glycerophosphocholine
GSH	Glutathione
JPRESS	J-resolved Point RESolved Spectroscopy
MCI	Mild cognitive impairment
MEGA PRESS	MEscher-GArwood Point RESolved Spectroscopy
mI	myo-Inositol
MRI	Magnetic resonance imaging
MRS	Magnetic resonance spectroscopy
NAA	*N*-Acetylaspartate
NAAG	*N*-Acetylaspartylglutamate
NMDA	*N*-Methyl-D-aspartic acid
NMR	Nuclear magnetic resonance
PCP	Phencyclidine
PC	Phosphorylcholine
PCr	Phosphocreatine
PET	Positron emission tomography
PRESS	Point RESolved Spectroscopy
RF	Radiofrequency
ROI	Region of interest
ROS	Reactive oxygen species
STEAM	STimulated Echo Acquisition Mode
SVS	Single voxel spectroscopy
TCA	Tricarboxylic acid cycle
TE	Echo time
TI	Inversion time
TR	Relaxation time

9.1 Magnetic Resonance Spectroscopy (MRS)

9.1.1 General Overview

Magnetic Resonance Spectroscopy (MRS) is a non-invasive technique that quantitatively measures the metabolic composition of tissues *in vivo* using conventional magnetic resonance (MR) scanners. This technology is of special interest for clinical applications in psychiatry due to its non-invasive nature. In recent years, studies have demonstrated its diagnostic capability in psychiatric conditions such as schizophrenia, bipolar disorder, depression, as well as in neurodegenerative disorders and neuro-oncology among others (Öz et al. 2014). The most relevant brain chemicals that can be quantified include: N-acetylaspartate (NAA), a neuronal marker; creatine (Cr), involved in energy metabolism; choline (Cho), a key component of myelin; glutamate (Glu), an excitatory neurotransmitter; γ-aminobutyric acid (GABA), an inhibitory neurotransmitter, and glutathione (GSH), an antioxidant involved in neuroinflammation. In this chapter, the biological roles of the primary brain metabolites will be discussed. Moreover, the general principles of MRS and the specialized pulse sequences that enable the detection each of these metabolites will be described. Furthermore, a comprehensive introduction of the most common techniques and examination protocols used in research and clinical applications will be presented.

9.1.2 Physics of MRS

MRS is based in nuclear magnetic resonance (NMR) spectroscopy, which was first introduced in the early 1950s and was typically employed in organic chemistry to define chemical structures (Bloch 1946; Bloch et al. 1946; Purcell et al. 1946). Shortly thereafter, NMR spectroscopy was successfully applied to the human body (Andrew 1980), providing access to quantitative and non-invasive studies of biochemistry.

The physics behind MRS is fundamentally the same as that utilized by NMR. In an MRS experiment, the patient is placed into a uniform static magnetic field such that unbound nuclei precess at

a specific frequency proportional to the field strength, known as the Larmor frequency. Then, a radiofrequency (RF) transmitter coil excites the nuclei by applying electromagnetic radiation in the form of an RF pulse. The nuclei absorb the electromagnetic energy, altering the orientation of the nuclear spins. Finally, as the nuclei relax back to their original state, energy is released and detected by the receiver in the RF coil as a free induction decay (FID) signal. By computing the Fourier transform of the measured FID, its spectral components can be obtained and visualized in a graph (Fig. 9.1). Each molecule in the sample resonates at established frequencies, which appear as a peak at a specific frequency location, or chemical shift, along the x-axis. The chemical shift of a molecule is often expressed in parts per million (ppm) of the Larmor frequency so the scale is independent of the magnetic field strength. In an MRS spectrum, the concentration of a specific metabolite is proportional to the area under the curve of each peak. Higher concentrations result in larger peaks, which enables MRS's use as a quantitative technique. Some pulse sequence parameters that largely influence the robustness and sensitivity of this technique are: echo time (TE), related to the time between the excitation and the signal readout; repetition time (TR), which corresponds to the time between consecutive excitations; number of signal averages and the volume of the excited tissue. The neurometabolites that can be detected with MRS are of great interest as they are tied to metabolic and neurological processes within the brain that directly relate to a physiological, cognitive or neuronal process.

9.1.3 Brain Metabolites

The abundance of hydrogen (^{1}H) in organic molecules and the relatively high sensitivity that it provides in MRS in comparison with other nuclei, allows detecting several characteristic resonances of the central nervous system (CNS). Although up to 18 metabolic components could be identified in a ^{1}H MRS spectrum *in vivo*, their detection is generally limited by different factors related to the hardware sensitivity, field strength, spectral overlap, signal artifacts, and patient stability. The present section presents a detailed description of the most relevant brain metabolites that can be reliably measured and quantified under healthy and disease conditions using clinical MR scanners, typically at 3 T magnetic field strength. In Fig. 9.1, a representative ^{1}H MRS examination is shown together with the measured spectrum and the different metabolic components present in it.

9.1.3.1 N-Acetyl Aspartate (NAA)

NAA is an amino-acid derivative synthesized in neurons and transported down axons (Moffett et al. 1993). In ^{1}H MRS of the brain and under healthy conditions, the primary resonance of NAA appears as the largest peak in the spectrum located at 2.02 ppm. Studies have also correlated the concentration of NAA in the brain with the number of neurons measured. Therefore, it is considered a marker of healthy neurons, axons, and dendrites (Urenjak et al. 1992). A diagnosis can be made using MRS by either comparing the numeric values of NAA concentrations or by recognizing abnormal patterns of peaks in the spectra. This has been shown across a variety of diseases (Lin et al. 2005; Harris et al. 2006; Moffett et al. 2007). Although different studies have shown some of the functions of NAA in the central nervous system, the main role of NAA is not fully understood (Barker 2001).

9.1.3.2 Creatine (Cr)

Creatine (Cr) and its phosphorylated version, phosphocreatine (PCr) appear with their major resonance at 3.02 ppm. The metabolism of Cr and PCr provides the basis of energy metabolism in the brain via the mitochondria where Cr is phosphorylated by the enzyme creatine kinase and adenosine triphosphate (ATP) to form PCr and vice-versa (Ross 2000). As a key metabolite to maintain energy homeostasis, Cr is uniform in different areas of the brain and between subjects. For this reason, the ratio to Cr is often reported as

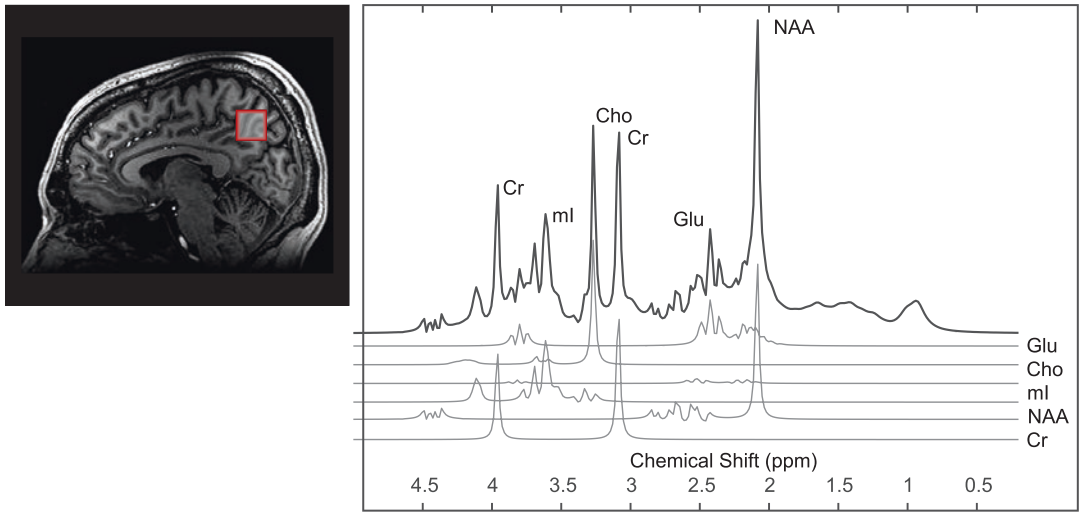

Fig. 9.1 Standard ^{1}H MRS of the brain at short echo time. (left) Selected volume of interest (VOI) within the brain showed together with the anatomical reference. (right) Measured spectrum containing resonances of five metabolites, namely glutamate (Glu), choline (Cho), myo-inositol (mI), N-acetyl-aspartate (NAA) and creatine (Cr)

a normalized concentration between metabolites and subjects. However, in some situations, energy utilization can be affected by disease and other Cr metabolic pathways, thus affecting the reliability of relative concentrations. Mitochondrial dysfunction in the brain would likely cause changes in Cr and PCr and has been implicated across a range of neuropsychiatric disorders including schizophrenia and bipolar disorder (Rezin et al. 2009). Cr can be also affected by osmotic equilibrium in the brain (Bluml et al. 1998). Furthermore, as Cr is synthetized in the liver, a reduction in Cr in the CNS can be caused by liver failure.

9.1.3.3 Choline (Cho)

Choline (Cho) or total Cho (tCho) includes several different metabolites: choline, phosphorylcholine (PC), and glycerophosphorylcholine (GPC), which are the main constituents, as well as phosphorylethanolamine and glycerophosphorylethanolamine, to a lesser extent. The primary resonance can be found at 3.2 ppm. These metabolites are components of the myelin sheath, crucial for the propagation of signals throughout the brain. As a result, an increased Cho level is found in areas of greater myelin and membrane density such as in the white matter. In addition, PC and GPC are involved in the metabolism of phosphatidylcholine and other membrane phospholipids. Thus, the turnover of the membrane of myelin phospholipids, as well as demyelination, are closely tied to increases in Cho as observed by MRS. Due to the involvement of Cho in both membrane turnover and degradation, as well as density, it is a sensitive but not necessarily a specific marker of membrane conditions.

Recent studies in Alzheimer's disease (Kantarci 2007), schizophrenia (Kraguljac et al. 2012), and depression (Caverzasi et al. 2012) have shown conflicting reports on Cho levels in these conditions. In bipolar disorder, however, the literature has shown a consistent elevated choline signal in the basal ganglia (Maddock and Buonocore 2012). The most likely reason for why Cho findings are discordant across different studies even within the same disease is due to the sensitivity of Cho to the gray and white matter volumes in the regions of interest studied. A solution to this problem is to combine image segmentation within the voxel of interest for MRS to account for the relative contributions of gray and white matter to the Cho level.

9.1.3.4 Myo-Inositol (mI)

Myo-inositol (mI) is a cyclic sugar-alcohol only detected at short echo times. Its main observable resonance peak appears at 3.52 ppm. mI is involved in a multitude of different metabolic processes (Ross and Bluml 2001), such as cerebral osmotic regulation and demyelination. While its role may not be well understood, the importance of mI, however, is the broad range of concentrations found across different diseases. For example, mI has nearly zero concentration in hepatic encephalopathy to up to a three-fold increase in newborns compared to nominal adult values. Therefore, it has been found to be highly specific and sensitive within the context of disease diagnosis in patients when compared with controls and therefore provides great clinical value.

Studies of dementia have highlighted the importance of mI. In the early stages of dementia, such as mild cognitive impairment (MCI), mI is elevated long before symptoms of dementia are obvious (Kantarci 2013). Moreover, in combination with NAA, mI predicts the outcome of MCI patients and is also highly sensitive and specific in the diagnosis of Alzheimer's disease (Öz et al. 2014).

9.1.3.5 Glutamate (Glu) and Glutamine (Gln)

Glu is an amino acid with several important roles in the human brain. It is the most abundant excitatory neurotransmitter; therefore, several neurological and psychiatric diseases have an impact upon this molecule. Neuronal dysfunction leads to an accumulation of Glu, which results in excitotoxicity. Additionally, Glu is a key compound in brain energy metabolism via the citric acid cycle. After its release into the synaptic cleft, Glu is taken up by adjoining cells through excitatory amino acid transporters. Astrocytes are responsible for uptake of most extracellular Glu preserving the low extracellular concentration of Glu needed for proper receptor-mediated functions (Schousboe 2003; Schousboe and Waagepetersen 2005). Glu is stored as Gln in the glial cells, and the balanced cycling between these two neurochemicals is essential for the normal functioning of brain cells (Gruetter et al. 1994; Mason et al. 1995).

Gln is the main precursor for neuronal Glu and GABA (Hertz and Zielke 2004). It has been estimated that the cycling between Gln and Glu accounts for more than 80% of cerebral glucose consumption (Sibson et al. 1998; Pellerin and Magistretti 1994). The molecular structures of Glu and Gln are very similar and, consequently, give rise to similar magnetic resonance spectra (Govindaraju et al. 2000). Thus, even though Glu has a relatively higher concentration in the brain, its major resonances are usually contaminated by contributions from Gln, GABA, GSH, and NAA. For this reason, the term Glx is often used to reflect the combined concentrations of Glu and Gln. Section 9.5 details different pulse sequences to achieve the separation of Glu from its neighboring metabolites.

9.1.3.6 γ-Amino Butyric Acid (GABA)

GABA is the major inhibitory neurotransmitter in the brain. In the developing brain, GABA is initially excitatory and later shifts to its inhibitory role as glutamatergic functions develop (Ben-Ari 2002). Moreover, GABA is of interest across a broad range of psychiatric conditions such as anxiety, memory loss, depression, and pain. GABA acts as an inhibitor by binding to specific receptors that open ion channels, creating a negative membrane potential and preventing the further formation of action potentials. Nevertheless, the detection of GABA using MRS is challenging due to a couple of reasons. First, the concentration of GABA in the brain is rather low, ranging from 1.3 to 1.9 mM (Govindaraju et al. 2000), therefore it is difficult to detect accurately and consistently. Additionally, GABA nuclear spins couple with other neighboring spins, causing the molecule to appear as multiple resonances around 1.9 ppm, 2.28 ppm, and 3.0 ppm, that overlap with other major metabolites such as NAA, Glu, and Cr, respectively. Therefore, specialized sequences (see Sects. 9.3.2 and 9.5) are required to reliably estimate GABA concentrations in vivo.

9.1.3.7 Glutathione (GSH)

The primary role of GSH is as an anti-oxidant, providing a defense system against oxidative stress (Dringen et al. 2000), which can cause

damage related to DNA modification, lipid peroxidation, and protein modification, from which the brain is especially vulnerable. Oxidative stress is also strongly associated with neuroinflammatory processes (Agostinho et al. 2010; Mosley et al. 2006). Consequently, GSH metabolism has been found to play an important role in the pathogenesis of neurodegenerative disorders, as well as psychiatric disorders. GSH is synthesized intracellularly and differently between neurons and glial cells, thus providing an interesting specificity to GSH measures to identify inflammatory processes.

GSH is composed of Glu, cysteine, and glycine, therefore its spectrum highly overlaps with all three of those metabolites (Matsuzawa and Hashimoto 2011). Particularly of concern is the overlap with Glu, given that GSH concentrations in the brain are 1–3 mM whereas Glu concentrations are 6–10 mM (Govindaraju et al. 2000). With minor modifications to the methods that will be described in Sects. 9.3.2 and 9.5, resonances of GSH can be effectively separated from Glu.

9.2 Localization Techniques

To detect and to quantify the metabolic components of brain tissue it is necessary to precisely localize the volume of interest (VOI) within the brain. To achieve this, RF pulses combined with magnetic gradients are used to selectively excite the given region of the brain. This effectively isolates the signal from the VOI avoiding overwhelming lipid signals from the skull that can contaminate the signal. In this section, three commonly used localization sequences will be described.

9.2.1 Stimulated Echo Acquisition Mode (STEAM)

STEAM is a method that uses a series of three consecutive slice-selective 90° pulses for localization (Frahm et al. 1989). Since the sequence only yields half as much of the maximum detectable magnetization, the signal-to-noise ratio (SNR) is reduced compared to other localization methods such as PRESS or semi-LASER. Nevertheless, an effective water suppression and shorter echo times (TE; the time between the first two 90° pulses and between the third 90° pulse and the stimulated echo) are more easily accomplished via STEAM (Haase et al. 1986). This provides an advantage when detecting short-T2 metabolites such as GABA, mI, Glu, and Gln.

9.2.2 Point-Resolved Spectroscopy (PRESS)

PRESS is a localization technique that selectively excites a specified volume using a pulse sequence that consists of a slice-selective 90° pulse followed by two slice-selective refocusing 180° pulses (Bottomley 1987). Each RF pulse is applied in conjunction with a perpendicular gradient. The first pulse excites an axial slice, while the other two pulses refocus the proton spins inside the intersection of the three perpendicular slices. In the selected volume, B_0-field homogeneity can be optimized using shim coils to improve the spectral line width and consequently the quality of the measurement. Reduction of contamination by nuisance signals, i.e., water and lipids, is often achieved by additional outer volume suppression (OVS) bands around the localized voxel. While this technique achieves a higher SNR than STEAM, it suffers from chemical shift displacement errors (Andronesi et al. 2010) that reduce the reliability of the localization at high field strengths. Similar to STEAM, metabolites with short T2 are not visible at longer echo times (TE > 80 ms) such that only NAA, Cr, and Cho can be measured.

9.2.3 Semi-Localized by Adiabatic Selective Refocusing (Semi-LASER)

Semi-LASER is an improved localization method that incorporates amplitude- and frequency-

modulated adiabatic full passage (AFP) refocusing pulses. The sequence utilizes an optimized 90° slice-selective pulse followed by a pair of 180° AFP slice selective refocusing pulses (Scheenen et al. 2008a; Scheenen et al. 2008b). The adiabatic pulses achieve an in-plane spin refocusing that is less sensitive to B_1-field inhomogeneities and chemical shift displacement errors, resulting in a more accurate localization. Nevertheless, due to the high energy that AFP pulses deposit in the subject, the minimum repetition time (TR) is limited, thus extending the total acquisition duration.

9.3 Single Voxel Spectroscopy (SVS)

The standard SVS experiment incorporates, at each TR, a water suppression module, a volume localization module and record the resulting FID. To improve SNR, several excitations are recorded and then averaged. Studies have shown that short-TE acquisitions increase the SNR and maximize the number of metabolic components that can be detected (Mlynárik et al. 2006). Details regarding signal reconstruction and processing will be described in Sect. 9.7.

9.3.1 TE-Averaged PRESS

In this method, a series of 1D PRESS spectra are measured with increasing TE value. Then the signals are averaged to produce a 1D spectrum that contains an average of the TE effects in the signal (Bolan et al. 2002; Dreher and Leibfritz 1995). From this 1D spectrum, relatively uncontaminated Glu and Glx peaks can be quantified (Hurd et al. 2004). While TE-averaging is a simple and reliable method for measuring Glu and Gln, it sacrifices spectral information arising from the J-evolution of other metabolites. Moreover, a different T2 effect is present at each TE value, which should be ideally corrected using a basis set with the same experimental parameters as the acquired sequence.

9.3.2 J-Editing

Spectral editing, or J-difference editing, is a method that enables the detection of resonances that overlap with higher-concentration metabolites. Some examples include GABA, which overlaps with Cr, and lactate, which can be obscured by the lipid signal. In general, this method applies the concept of scalar coupling to modify the signal of a single scalar-coupled metabolite and separates it from uncoupled metabolites (Rothman et al. 1984).

9.3.2.1 Meshcher-Garwood PRESS (MEGA-PRESS)

In MEGA-PRESS (Mullins et al. 2014), the J-editing method introduced in the previous section is used in combination with the PRESS excitation scheme. Currently, this technique is widely used as the standard for GABA editing. GABA has two characteristic resonances at 3.0 ppm and 1.9 ppm. Applying a frequency-selective pulse that is on resonance at 1.9 ppm would increase the signal in the 3.0 ppm region if GABA is indeed present. Likewise, a frequency-selective pulse that is off resonance would not influence the 3.0 ppm peak. Subtracting the spectra from these two different acquisitions should preserve the metabolite that only resonates at the characteristic frequencies of GABA. Although this method has shown to successfully estimate GABA concentrations in several brain regions including the anterior cingulate cortex, occipital lobe, and parietal lobe (Terpstra et al. 2002; Öz et al. 2006; Bhattacharyya et al. 2007; Waddell et al. 2007; Kaiser et al. 2007; Edden and Barker 2007), spectral subtraction may lead to artifacts or loss in SNR and undesired off-resonance effects may affect the robustness of the technique.

9.4 Chemical Shift Imaging (CSI)

Chemical shift imaging (CSI), also known as MR spectroscopic imaging (MRSI), allows measuring the spatial distribution of metabolites in the brain. Like in MRI, magnetic gradients are used

to encode the 2D or 3D frequency components of the sample, known as k-space. Like SVS, localization using STEAM, PRESS or semi-LASER and water suppression modules are typically used in combination with the spatial encoding to reduce artifacts related to nuisance signals. For each phase encode, the spectral information is acquired in the form of an FID. Therefore, the signal can be reconstructed following the pipeline described in Fig. 9.2, with the incorporation of an additional 2D or 3D Fourier transform. The reconstructed data can be then visualized as an intensity map showing the spatial distribution of each metabolite. This map is typically interpolated and overlaid with the anatomical MRI image as shown in Fig. 9.3a, b. Alternatively, the reconstructed spectra can be visualized in a grid (Fig. 9.3c) to evaluate its features and detect potential artifacts in the signal, thus avoiding misinterpretation of the data.

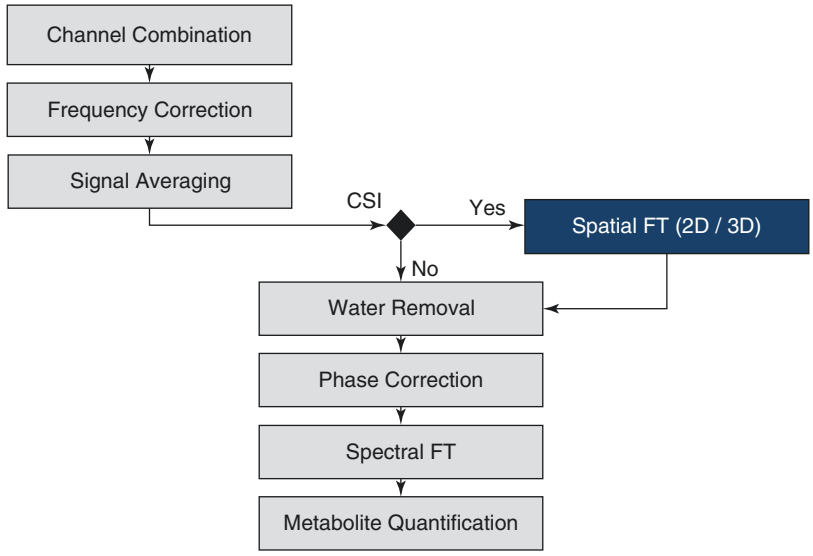

Fig. 9.2 Standard reconstruction and processing pipeline for ^{1}H MRS experiments. Equivalent reconstruction steps can be used for SVS and CSI with only of one extra processing step involved in computing the 2D or 3D spatial Fourier transform (FT) of the data (blue)

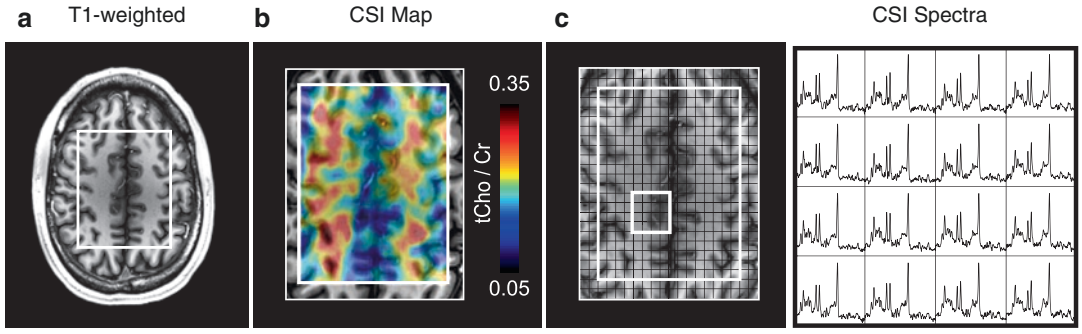

Fig. 9.3 Visualization of 2D CSI reconstructed data. (**a**) The corresponding anatomical T1-weighted image and the localized voxel. (**b**) A representative metabolite map showing the distribution of the total choline to creatine ratio (tCho/Cr). (**c**) Local CSI spectra displayed in every voxel for qualitative assessment. (Modified from Coello et al. 2018)

In CSI acquisitions, the optimization of the B_0-homogeneity is challenging due to the large volume that is measured. This reduces the spectral resolution and may cause spectral overlapping and inaccuracies in metabolite quantification. Moreover, the spatial information measured can extend the acquisition time considerably, limiting the maximum resolution of 2D and 3D-CSI.

9.4.1 Phase Encoded CSI

Phase encoded CSI is the most widely used due to its simplicity and SNR efficiency. It uses magnetic gradients to additionally encode the spatial dimensions of the measured sample. Then the FID signal is recorded in the absence of any gradient to preserve the spectroscopic information. Each voxel in the acquired VOI contains a spectrum that allows for the assessment of the metabolic profile of a specific location or alternatively for the visualization of the spatial distribution of a specific metabolite of interest. This has an advantage over single voxel MRS techniques, as multiple brain regions can be assessed using the CSI technique. However, the acquisition time directly scales with the number of phase encodes, i.e., the number of spatial positions encoded, which limit the maximum matrix size that can be acquired in a clinically feasible time. Several alternatives to phase encoded CSI have been proposed to either reduce scan time or increase the spatial resolution. These include spiral phase encoding, echo-planar sequences, multi-slice sequences, and parallel imaging methods (Posse et al. 2013).

9.4.2 Echo Planar Spectroscopic Imaging (EPSI)

Fast encoding-efficient techniques such as EPSI shorten the acquisition time of CSI scans at the cost of SNR (Posse et al. 1995; Posse et al. 1994). Based on the same principle as echo planar imaging (EPI), this technique simultaneously encodes and acquires the temporal dimension and one spatial dimension. This is achieved using an oscillating gradient that encodes one spatial dimension during the sampling of the FID. Two gradient trajectories commonly used are flyback and symmetric EPSI readouts. In flyback EPSI (Cunningham et al. 2005), sampling takes place only during positive lobes of the oscillating gradient. This has the advantage of being more robust against trajectory imperfections since the flyback gradient causes the sampling points to be well aligned. However, this approach requires a high gradient performance and a significant amount of time is spent on the flyback segment of the trajectory. In symmetric EPSI (Zierhut et al. 2009), on the other hand, the readout takes place during both positive and negative gradient segments. This provides enhanced SNR efficiency and is less gradient demanding. Nonetheless, the bipolar trajectory is prone to spectral ghosting artifacts due to inconsistencies between the odd and even k-space lines, which requires an extra correction step (Coello et al. 2018).

9.5 Two-Dimensional Spectroscopy

Two-dimensional and multi-dimensional spectroscopy methods make it possible to separate scalar coupled and noncoupled metabolites into orthogonal planes (Aue et al. 1976). Despite the longer measurement times compared to 1D MRS, 2D spectroscopic techniques have a great potential for the unambiguous detection of overlapping frequencies. Thus, increasing the number of metabolites that can be reliably quantified.

9.5.1 Correlation Spectroscopy (COSY)

2D correlation spectroscopy (COSY) utilizes a sequence with two 90° pulses separated by a time interval t_1, with variable increments between consecutive excitations, and with a standard readout

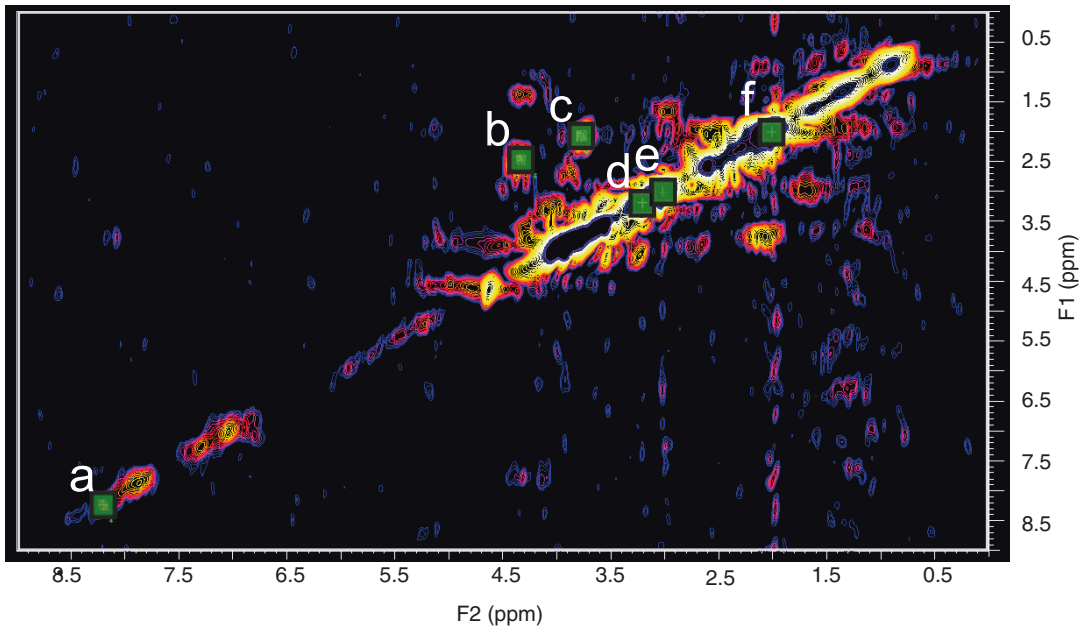

Fig. 9.4 Reconstructed 2D COSY spectrum. Green squares indicate the location of six metabolic components of interest, namely (**a**) GSH, (**b**) NAA, (**c**) Glx, (**d**) Cho, (**e**) Cr, and (**f**) NAA. Quantification can be performed by integration of the area under the peak of interest relative to the area of Cr

time t_2. In this way, a series of 1D spectra is acquired (Jeener et al. 1979). After two-dimensional Fourier transform (FT) of the time dimensions t_1 and t_2, a 2D spectrum is obtained. Figure 9.4 shows a typical reconstructed COSY spectrum, where the x and y axes correspond to the frequencies F2 and F1, respectively. In 2D COSY, scalar-coupling between protons in molecules results in cross-peaks that allow for unambiguous identification of different metabolites (Thomas et al. 2001; Cocuzzo et al. 2011; Ramadan et al. 2011). This technology has been translated to clinical MR scanners and has been applied in vivo (Schulte et al. 2006), demonstrating detection of GABA, Glu, Gln, GSH, among other metabolites (Figs. 9.4 and 9.5).

9.5.2 2D JPRESS

2D JPRESS acquires a series of TE increments to provide a 2D MR spectrum. It differs from 2D COSY in that it utilizes the standard PRESS sequence for each increment with the addition of a maximum echo sampling scheme. This approach increases the sensitivity of the method (Schulte et al. 2006; Ke et al. 2000; Lymer et al. 2007). However, an additional consideration is also necessary to quantify the 2D JPRESS spectra. Unlike COSY where the cross-peak volumes can be measured as an analog of metabolite concentration, 2D JPRESS cross-peaks are not as differentiated and therefore this method does not lend itself as readily for visual analysis. Tools for the quantification of this type of data, like ProFit (Schulte and Boesiger 2006), use prior knowledge, i.e., simulated basis sets of the metabolites, to perform a non-linear fit of the 2D spectrum. In addition, 2D-JPRESS can be combined with the CSI acquisitions described in Sect. 9.4 (Jensen et al. 2005). 2D-JPRESS CSI can sample the distribution of metabolite concentrations throughout the brain. However, this considerably reduces SNR and extends the acquisition time thus making it challenging to obtain reliable estimates for low-concentration metabolites, such as GABA or GSH.

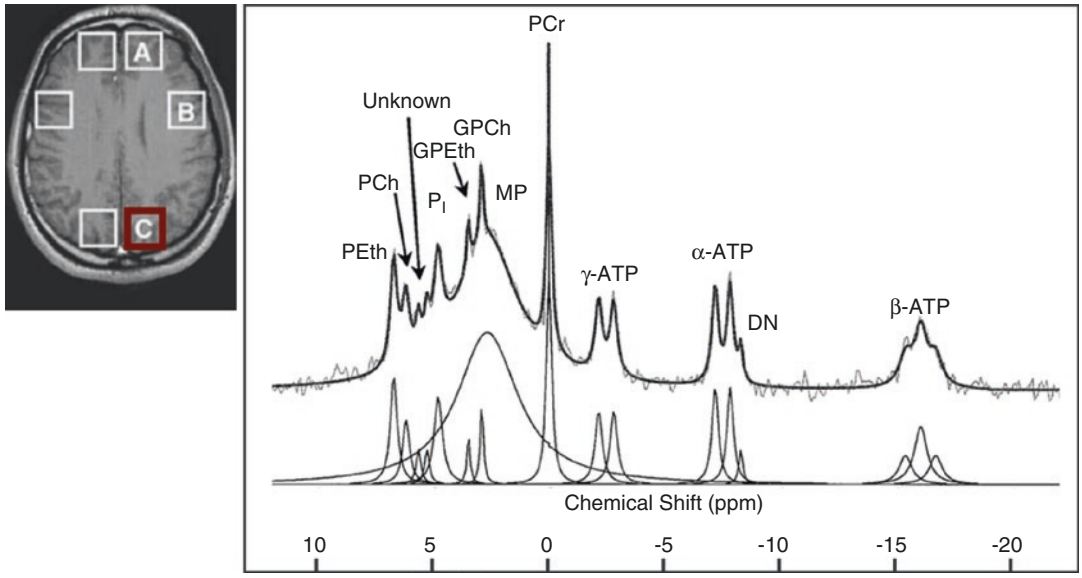

Fig. 9.5 ^{31}P brain spectrum measured with 2D CSI. The location of the plotted spectrum is indicated in red. The right plot shows the measured signal and the spectral fit, where the principal resonances can be identified. (Modified from Potwarka et al. 1999)

9.6 Multi-nuclear Spectroscopy

In addition to ^{1}H MRS, NMR-detectable nuclei that form biomolecules include phosphorous 31, carbon 13 and sodium 23, among others. For several CNS applications, these isotopes are shown to be highly specific and sensitive to changes. Despite the differences in the spectral appearance, resonances that can be found, and measurement challenges that are specific to each of the NMR-detectable nuclei (described in the detail below), the basic principles of the technique, signal acquisition and processing remain unchanged.

9.6.1 Phosphorus-31 (^{31}P) Spectroscopy

^{31}P MRS can be used to qualify brain energetics by measuring the ^{31}P signal from phosphocreatine as well as inorganic phosphate, adenosine triphosphate, and phospholipids such as phosphoethanolamine and phosphocholine, as well as glycerophosphoethanolamine and glycerophosphocholine. ^{31}P studies have focused on reduced PCr in schizophrenia (Blüml et al. 1999; Kegeles et al. 1998), which supports findings from proton MRS studies where reduced Cr has been found using TE-averaged PRESS (Ongür et al. 2009). In the same study, bipolar disorder did not show changes in PCr, however, other studies using both proton MRS (Frey et al. 2007) and ^{31}P MRS (Kato et al. 1994) have shown reductions in Cr and PCr. Findings of changes in Cr in schizophrenia and bipolar disorder are inconsistent. A recent study showed that meta-analysis failed to find significant abnormalities in Cr levels in both diseases (Kraguljac et al. 2012). Other techniques used to measure neurological changes using ^{31}P MRS include diffusion tensor spectroscopy (DTS) (Du et al. 2013) and phosphorus magnetization transfer (MT) (Du et al. 2014).

9.6.2 Carbon (^{13}C) Spectroscopy

Unlike ^{31}P MRS, which focuses on the inherent metabolites within the brain, ^{13}C MRS takes advantage of the low background levels of natural abundance ^{13}C (1.1%) in order to provide

high contrast when ^{13}C-labelled substrates such as ^{13}C-1-glucose or acetate are infused. This allows for the measurement of the metabolites that are subsequently labeled by the metabolism of the substrates. Of particular interest for psychiatry is the ability to measure glutamate and glutamine synthesis rates as a putative measure of neurotransmission. While there have been very limited studies in schizophrenia (Harris et al. 2006), this would prove to be a fascinating area of research.

9.7 MRS Signal Processing

This section outlines data reconstruction and processing as it is generally used for spectroscopic data. Figure 9.2 shows the pipeline of standard data processing applicable to SVS and CSI datasets. Often, a water reference scan is acquired in addition to the water-suppressed metabolite scan, which can be used to further process the spectral data. In the following sections, the processing steps are explained.

9.7.1 SVS Reconstruction

In SVS a complex 1D temporal signal, known as FID, is measured using single- or multi-channel receiver coils in a single TR. Then, the process is repeated to increase SNR via signal averaging. Therefore, several processing steps are required to retrieve a single spectrum from the multi-dimensional signal recorded. Initially, the measurement of each of the coils in the multi-channel receiver is combined. This can be done by simple averaging after signal phasing or using singular value decomposition (SVD) to obtain weighting factors proportional to the signal intensity in each channel, which optimizes the SNR of the combined signal. Then, frequency shifts in the signal, caused by temperature changes or B_0-drifts are corrected through the alignment of the different repetitions before averaging them. This coherently adds the signals and improves the full width at half maximum (FWHM), i.e., the spectral resolution. Finally, the large water signal and zero-order phase are removed from the single 1D temporal signal and the spectrum is obtained via 1D Fourier transform.

9.7.2 CSI Reconstruction

In CSI acquisitions, additional dimensions related to the spatial information of the subject are measured using phase encoding. Analogous to MRI, this spatial information in arranged in a 2D or 3D k-space. In general, the processing steps to reconstruct such a signal are equivalent to the SVS pipeline. However, an additional spatial 2D or 3D FT is necessary to recover the spatial distribution of the signal. Figure 9.2 shows the position in the pipeline where the spatial transform is performed.

9.7.3 Post-processing

MRS data can be post-processed and analyzed in several ways. All major MR platforms have their own methods of reconstructing the data where the details are somewhat different, but the end result is generally an automated or semi-automated fitting of the metabolite peaks and a quantitative measure of major metabolites (NAA, creatine, choline, myo-inositol), usually as a ratio to creatine to provide a normalization factor to account for differences in the peak area or amplitude between subjects, which will differ depending on parameters such as the voxel size, number of averages, transmit/receiver gain, etc.

9.7.3.1 Water Signal Removal

As the metabolites to be detected exist at much lower concentrations, typically 3–4 orders of magnitude, water suppression during data acquisition is a key component of most MRS techniques. However, the intensity of the residual

water peak can still corrupt the baseline of the spectrum. Thus, it is necessary to remove further this unwanted residual water. This can be performed using Hankel singular value decomposition (HSVD). This method decomposes the temporal signal into decaying sinusoids and estimates the components of the water resonance peak (Barkhuijsen et al. 1987). By selecting the spectral range of the water peak, its corresponding FID can be fitted and then subtracted from the initial time domain signal. Finally, after Fourier transform, only the metabolite resonances remain in the spectrum.

9.7.3.2 Eddy Current Correction

Eddy currents are present in every measurement due to the interaction of magnetic field gradients with the scanner hardware components. These can introduce phase distortions in the spectrum and destroy the metabolite resonance peaks, especially in the range from 4.5 to 3.5 ppm. A methodology for correcting eddy current effects has been effectively demonstrated and widely used in vivo (Klose 1990). This method estimates the phase distortions from a water reference acquisition with identical sequence parameters but without water suppression. The estimated phase is then subtracted from the water-suppressed measurement in the time domain and the corrected spectrum is recovered via FT.

9.7.3.3 Frequency Shift Correction

During the acquisition of signal averages, fluctuations in the B_0-field may affect the center frequency of the measurement. This causes the center frequency of the measurement to drift through time and consequently, it blurs the spectral peaks when computing the average. Therefore, the alignment of every individual average is necessary to reduce the effects of the B_0-drifts and improve spatial resolution. It has been shown that when SVS is combined in the same clinical study with other gradient-intense sequences such as diffusion tensor imaging (DTI) this approach reduces the instability artifacts and improves the quantification of metabolites (Rowland et al. 2017).

9.8 Metabolite Quantification

Quantitative MRS is achieved by estimating the relative area of the resonance peaks, which is proportional to their concentration in the tissue. The MRS data can be exported before or after post-processing to be quantified using commercially available packages such as LCModel (Provencher 1993), jMRUI (Naressi et al. 2001), Tarquin (Wilson et al. 2011), AMARES (Vanhamme et al. 1997), etc. These software tools incorporate post-processing routines and prior knowledge to estimate the concentration of metabolites together with other quality measures, such as FWHM, SNR and error estimates.

9.8.1 LCModel Quantification

Fitting algorithms based on prior knowledge have shown superior robustness to non-liner distortions present in the spectra, such as eddy currents, distortions in the baseline, linear and zero-phase effects (de Graaf 2007). Most of these tools are based on modeling the fitting problem as a linear combination of a basis set generated via simulations, signal models or high-quality measurements following identical experimental conditions. LCModel is a widely used tool for used for quantification and reporting of SVS and CSI data. The fitting algorithm estimates the metabolite signal and separates it from the baseline component and the noise. Moreover, a list of the absolute concentrations, relative concentrations and Cramer-Rao Lower Bounds (CRLB) are computed for each metabolite present in the basis set. Finally, a summary of the results is obtained to perform a diagnosis and can be exported for further statistical analysis (Fig. 9.6).

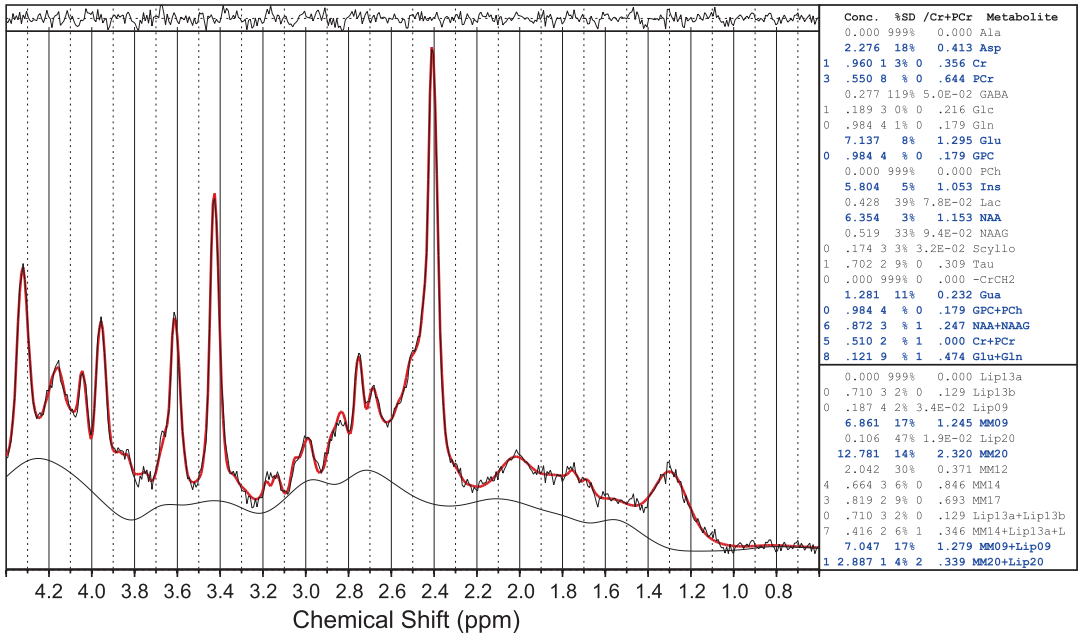

Fig. 9.6 Obtained report using LCModel quantification software (Provencher 1993). The spectral fit using a simulated metabolite basis set estimates the spectral fit (red) of the signal and residual components such as baseline and noise (black). Furthermore, the concentration values, relative concentrations (i.e. Cr ratio) and the CramerRao-Lower Bound (CRLB) are generated for each metabolite in the basis set

Summary

- Magnetic resonance spectroscopy (MRS) can non-invasively measure the concentration of brain metabolites that provide pathophysiological insight into neuropsychiatric diseases such as:
  - N-acetyl aspartate: neuronal marker
  - Creatine: energy marker
  - Choline: membrane marker
  - Myo-inositol: glial marker
  - Glutamate/glutamine: excitatory neurotransmission
  - Gamma-Amino Butyric Acid: inhibitory neurotransmission
  - Glutathione: neuroinflammation marker
- There are several different ways that MRS data can be acquired:
  - Localization methods such as STEAM, PRESS, and semi-LASER
  - Two dimensions providing increased spatial resolution
  - Two dimensions providing increased spectral resolution
  - Multinuclear (i.e., phosphorous) acquisitions
- The methods used for post-processing the MRS data also has an impact on the accuracy of the measurement:
  - Presenting 1D spatial spectral data
  - Presenting 2D spatial spectral data
  - Additional post-processing necessary to correct spectra
  - Quantitation of brain metabolites

References

Agostinho P, Cunha RA, Oliveira C, et al. Curr Pharm Des. 2010;16(25):2766–78.

Andrew ER. N.m.r. imaging of intact biological systems. Philos Trans R Soc Lond B Biol Sci. 1980;289(1037):471–81.

Andronesi OC, Ramadan S, Ratai EM, Jennings D, Mountford CE, Sorensen AG. Spectroscopic imaging with improved gradient modulated constant adiabaticity pulses on high-field clinical scanners. J Magn Reson [Internet]. 2010;203(2):283–93. https://doi.org/10.1016/j.jmr.2010.01.010.

Aue WP, Bartholdi E, Ernst RR. Two-dimensional spectroscopy. Application to nuclear magnetic resonance. J Chem Phys [Internet]. 1976;64(5):2229–46. https://doi.org/10.1063/1.432450.

Barker PB. N-acetyl aspartate--a neuronal marker? Ann Neurol. 2001;49(4):423–4.

Barkhuijsen H, de Beer R, van Ormondt D. Improved algorithm for noniterative time-domain model fitting to exponentially damped magnetic resonance signals. J Magn Reson [Internet]. 1987;73(3):553–7. http://linkinghub.elsevier.com/retrieve/pii/0022236487900230.

Ben-Ari Y. Excitatory actions of gaba during development: the nature of the nurture. Nat Rev Neurosci. 2002;3(9):728–39.

Bhattacharyya PK, Lowe MJ, Phillips MD. Spectral quality control in motion-corrupted single-voxel J-difference editing scans: an interleaved navigator approach. Magn Reson Med. 2007;58(4):808–12.

Bloch F. Nuclear induction. Phys Rev [Internet]. 1946;70(7–8):460–74. https://link.aps.org/doi/10.1103/PhysRev.70.460.

Bloch F, Hansen WW, Packard M. The nuclear induction experiment. Phys Rev [Internet]. 1946;70(7–8):474–85. https://link.aps.org/doi/10.1103/PhysRev.70.474.

Bluml S, Zuckerman E, Tan J, Ross BD. Proton-decoupled 31P magnetic resonance spectroscopy reveals osmotic and metabolic disturbances in human hepatic encephalopathy. J Neurochem. 1998;71(4):1564–76.

Blüml S, Tan J, Harris K, Adatia N, Karme A, Sproull T, et al. Quantitative proton-decoupled 31P MRS of the schizophrenic brain in vivo. J Comput Assist Tomogr. 1999;23(2):272–5.

Bolan PJ, DelaBarre L, Baker EH, Merkle H, Everson LI, Yee D, et al. Eliminating spurious lipid sidebands in 1H MRS of breast lesions. Magn Reson Med. 2002;48:215–22.

Bottomley PA. Spatial localization in NMR spectroscopy in vivo. Ann N Y Acad Sci [Internet]. 1987;508:333–48. https://doi.org/10.1111/j.1749-6632.1987.tb32915.x.

Caverzasi E, Pichiecchio A, Poloni GU, Calligaro A, Pasin M, Palesi F, et al. Magnetic resonance spectroscopy in the evaluation of treatment efficacy in unipolar major depressive disorder: a review of the literature. Funct Neurol. 2012;27(1):13–22.

Cocuzzo D, Lin A, Ramadan S, Mountford C, Keshava N. Algorithms for characterizing brain metabolites in two-dimensional in vivo MR correlation spectroscopy. Conf Proc IEEE Eng Med Biol Soc. 2011;2011:4929–34.

Coello E, Noeske R, Burns BL, Gordon JW, Jakary A, Menze B, et al. High-resolution echo-planar spectroscopic imaging at ultra-high field. NMR Biomed [Internet]. 2018:e3950. https://doi.org/10.1002/nbm.3950.

Cunningham CH, Vigneron DB, Chen AP, Xu D, Nelson SJ, Hurd RE, et al. Design of flyback echo-planar readout gradients for magnetic resonance spectroscopic imaging. Magn Reson Med. 2005;54(5):1286–9.

Dreher W, Leibfritz D. On the use of 2-Dimensional-J NMR measurements for in-vivo proton MRS- measurement of homonuclear decoupled spectra without the need for short echo times. Magn Reson Med. 1995;34(3):331–7.

Dringen R, Gutterer JM, Hirrlinger J. Glutathione metabolism in brain. Eur J Biochem. 2000;267(16):4912–6.

Du F, Cooper AJ, Thida T, Shinn AK, Cohen BM, Öngür D. Myelin and axon abnormalities in schizophrenia measured with magnetic resonance imaging techniques. Biol Psychiatry [Internet]. 2013;74(6):451–7. http://www.ncbi.nlm.nih.gov/pmc/articles/PMC3720707/.

Du F, Cooper AJ, Thida T, Sehovic S, Lukas SE, Cohen BM, et al. In vivo evidence for cerebral bioenergetic abnormalities in schizophrenia measured using 31 P magnetization transfer spectroscopy. JAMA Psychiatry [Internet]. 2014;71(1):19. +.

Edden RAE, Barker PB. Spatial effects in the detection of γ-aminobutyric acid: improved sensitivity at high fields using inner volume saturation. Magn Reson Med. 2007;58(6):1276–82.

Frahm J, Bruhn H, Gyngell ML, Merboldt KD, Hänicke W, Sauter R. Localized high-resolution proton NMR spectroscopy using stimulated echoes: initial applications to human brain in vivo. Magn Reson Med. 1989;9(1):79–93.

Frey BN, Stanley JA, Nery FG, Monkul ES, Nicoletti MA, Chen H-H, et al. Abnormal cellular energy and phospholipid metabolism in the left dorsolateral prefrontal cortex of medication-free individuals with bipolar disorder: an in vivo 1H MRS study. Bipolar Disord. 2007;9(Suppl 1):119–27.

Govindaraju V, Young K, Maudsley AA. Proton NMR chemical shifts and coupling constants for brain metabolites. NMR Biomed [Internet]. 2000;13:129–53. http://www.ncbi.nlm.nih.gov/entrez/query.fcgi?cmd=Retrieve&db=PubMed&dopt=Citation&list_uids=10861994.

de Graaf RA. In vivo NMR spectroscopy - principles and techniques. 2nd ed. Hoboken: Wiley; 2007.

Gruetter R, Novotny EJ, Boulware SD, Mason GF, Rothman DL, Shulman GI, et al. Localized 13C NMR spectroscopy in the human brain of amino acid labeling from d-[1-13C]glucose. J Neurochem. 1994;63(4):1377–85.

Haase A, Frahm J, Matthaei D, Hänicke W, Bomsdorf H, Kunz D, et al. MR imaging using stimulated echoes (STEAM). Radiology. 1986;160(3):787–90.

Harris K, Lin A, Bhattacharya P, Tran T, Wong W, Ross B. Regulation of NAA-synthesis in the human brain in vivo: Canavan's disease, Alzheimer's disease and schizophrenia. In: N-Acetylaspartate [Internet]. New York: Springer; 2006. p. 263–73. http://link.springer.com/10.1007/0-387-30172-0_18.

Hertz L, Zielke HR. Astrocytic control of glutamatergic activity: astrocytes as stars of the show. Trends Neurosci. 2004;27(12):735–43.

Hurd R, Sailasuta N, Srinivasan R, Vigneron DB, Pelletier D, Nelson SJ. Measurement of brain glutamate using TE-averaged PRESS at 3T. Magn Reson Med. 2004;51(3):435–40.

Jeener J, Meier BH, Bachmann P, Ernst RR. Investigation of exchange processes by two-dimensional NMR spectroscopy. J Chem Phys. 1979;71(11):4546.

Jensen JE, Frederick BD, Wang L, Brown J, Renshaw PF. Two-dimensional, J-resolved spectroscopic imaging of GABA at 4 Tesla in the human brain. Magn Reson Med. 2005;54(4):783–8.

Kaiser LG, Young K, Matson GB. Elimination of spatial interference in PRESS-localized editing spectroscopy. Magn Reson Med. 2007;58(4):813–8.

Kantarci K. 1H magnetic resonance spectroscopy in dementia. Br J Radiol. 2007;80 Spec No:S146–52.

Kantarci K. Proton MRS in mild cognitive impairment. J Magn Reson Imaging. 2013;37(4):770–7.

Kato T, Takahashi S, Shioiri T, Murashita J, Hamakawa H, Inubushi T. Reduction of brain phosphocreatine in bipolar II disorder detected by phosphorus-31 magnetic resonance spectroscopy. J Affect Disord. 1994;31(2):125–33.

Ke Y, Cohen BM, Bang JY, Yang M, Renshaw PF. Assessment of GABA concentration in human brain using two-dimensional proton magnetic resonance spectroscopy. Psychiatry Res. 2000;100(3):169–78.

Kegeles LS, Humaran TJ, Mann JJ. In vivo neurochemistry of the brain in schizophrenia as revealed by magnetic resonance spectroscopy. Biol Psychiatry. 1998;44(6):382–98.

Klose U. In vivo proton spectroscopy in presence of eddy currents. Magn Reson Med [Internet]. 1990;14(1):26–30. http://www.ncbi.nlm.nih.gov/pubmed/2161984.

Kraguljac NV, Reid M, White D, Jones R, den Hollander J, Lowman D, et al. Neurometabolites in schizophrenia and bipolar disorder - a systematic review and meta-analysis. Psychiatry Res. 2012;203(2–3):111–25.

Lin A, Ross BD, Harris K, Wong W. Efficacy of proton magnetic resonance spectroscopy in neurological diagnosis and neurotherapeutic decision making. NeuroRx. 2005;2(2):197–214.

Lymer K, Haga K, Marshall I, Sailasuta N, Wardlaw J. Reproducibility of GABA measurements using 2D J-resolved magnetic resonance spectroscopy. Magn Reson Imaging. 2007;25(5):634–40.

Maddock RJ, Buonocore MH. MR spectroscopic studies of the brain in psychiatric disorders. Curr Top Behav Neurosci. 2012;11:199–251.

Mason GF, Gruetter R, Rothman DL, Behar KL, Shulman RG, Novotny EJ. Simultaneous determination of the rates of the TCA cycle, glucose utilization, μ-ketoglutarate/glutamate exchange, and glutamine synthesis in human brain by NMR. J Cereb Blood Flow Metab. 1995;15(1):12–25.

Matsuzawa D, Hashimoto K. Magnetic resonance spectroscopy study of the antioxidant defense system in schizophrenia. Antioxid Redox Signal. 2011;15(7):2057–65.

Mlynárik V, Gambarota G, Frenkel H, Gruetter R. Localized short-echo-time proton MR spectroscopy with full signal-intensity acquisition. Magn Reson Med [Internet]. 2006;56(5):965–70. https://doi.org/10.1002/mrm.21043.

Moffett JR, Namboodiri MA, Neale JH. Enhanced carbodiimide fixation for immunohistochemistry: application to the comparative distributions of N-acetylaspartylglutamate and N-acetylaspartate immunoreactivities in rat brain. J Histochem Cytochem. 1993;41(4):559–70.

Moffett JR, Ross B, Arun P, Madhavarao CN, Namboodiri AMA. N-Acetylaspartate in the CNS: from neurodiagnostics to neurobiology. Prog Neurobiol. 2007;81(2):89–131.

Mosley RL, Benner EJ, Kadiu I, Thomas M, Boska MD, Hasan K, et al. Neuroinflammation, oxidative stress and the pathogenesis of Parkinson's disease. Clin Neurosci Res. 2006;6(5):261–81.

Mullins PG, McGonigle DJ, O'Gorman RL, Puts NAJ, Vidyasagar R, Evans CJ, et al. Current practice in the use of MEGA-PRESS spectroscopy for the detection of GABA. Neuroimage. 2014;86:43–52.

Naressi A, Couturier C, Castang I, de Beer R, Graveron-Demilly D. Java-based graphical user interface for MRUI, a software package for quantitation of in vivo/medical magnetic resonance spectroscopy signals. Comput Biol Med [Internet]. 2001;31(4):269–86. http://www.sciencedirect.com/science/article/pii/S0010482501000063.

Ongür D, Prescot AP, Jensen JE, Cohen BM, Renshaw PF. Creatine abnormalities in schizophrenia and bipolar disorder. Psychiatry Res. 2009;172(1):44–8.

Öz G, Terpstra M, Tkáč I, Aia P, Lowary J, Tuite PJ, et al. Proton MRS of the unilateral substantia nigra in the human brain at 4 tesla: detection of high GABA concentrations. Magn Reson Med. 2006;55(2):296–301.

Öz G, Alger JR, Barker PB, Bartha R, Bizzi A, Boesch C, et al. Clinical proton MR spectroscopy in central nervous system disorders. Radiology [Internet]. 2014;270(3):658–79. http://pubs.rsna.org/doi/10.1148/radiol.13130531.

Pellerin L, Magistretti P. Glutamate uptake into astrocytes stimulates aerobic glycolysis: a mechanism coupling neuronal activity to glucose utilization. Proc Natl Acad Sci U S A. 1994;91:10625–9.

Posse S, DeCarli C, Le Bihan D. Three-dimensional echo-planar MR spectroscopic imaging at short echo times in the human brain. Radiology [Internet]. 1994;192(3):733–8. http://pubs.rsna.org/doi/abs/10.1148/radiology.192.3.8058941.

Posse S, Tedeschi G, Risinger R, Ogg R, Le Bihan D. High speed 1H spectroscopic imaging in human brain by echo planar spatial-spectral encoding. Magn Reson Med. 1995;33(1):34–40.

Posse S, Otazo R, Dager SR, Alger J. MR spectroscopic imaging: principles and recent advances. J Magn Reson Imaging. 2013;37(6):1301–25.

Potwarka JJ, Drost DJ, Williamson PC, Carr T, Canaran G, Rylett WJ, et al. A 1H-decoupled 31P chemical shift imaging study of medicated schizophrenic patients and healthy controls. Biol Psychiatry [Internet]. 1999;45(6):687–93. http://linkinghub.elsevier.com/retrieve/pii/S000632239800136X

Provencher SW. Estimation of metabolite concentrations from localized in vivo proton NMR spectra. Magn Reson Med [Internet]. 1993;30(6):672–9. http://www.ncbi.nlm.nih.gov/pubmed/8139448.

Purcell EM, Torrey HC, Pound RV. Resonance absorption by nuclear magnetic moments in a solid. Phys Rev [Internet]. 1946;69(1–2):37–8. https://link.aps.org/doi/10.1103/PhysRev.69.37.

Ramadan S, Andronesi OC, Stanwell P, Lin AP, Sorensen AG, Mountford CE. Use of in vivo two-dimensional MR spectroscopy to compare the biochemistry of the human brain to that of glioblastoma. Radiology. 2011;259(2):540–9.

Rezin GT, Amboni G, Zugno AI, Quevedo J, Streck EL. Mitochondrial dysfunction and psychiatric disorders. Neurochem Res. 2009;34(6):1021–9.

Ross BD. Real or imaginary? Human metabolism through nuclear magnetism. IUBMB Life. 2000;50(3):177–87.

Ross B, Bluml S. Magnetic resonance spectroscopy of the human brain. Anat Rec. 2001;265(2):54–84.

Rothman DL, Behar KL, Hetherington HP, Shulman RG. Homonuclear 1H double-resonance difference spectroscopy of the rat brain in vivo. Proc Natl Acad Sci [Internet]. 1984;81(20):6330–4. http://www.pnas.org/cgi/doi/10.1073/pnas.81.20.6330.

Rowland BC, Liao H, Adan F, Mariano L, Irvine J, Lin AP. Correcting for frequency drift in clinical brain MR spectroscopy. J Neuroimaging [Internet]. 2017;27(1):23–8. https://doi.org/10.1111/jon.12388.

Scheenen TWJ, Klomp DWJ, Wijnen JP, Heerschap A. Short echo time 1H-MRSI of the human brain at 3T with minimal chemical shift displacement errors using adiabatic refocusing pulses. Magn Reson Med. 2008a;59(1):1–6.

Scheenen TW, Heerschap A, Klomp DW. Towards 1H-MRSI of the human brain at 7T with slice-selective adiabatic refocusing pulses. MAGMA. 2008b;21(1–2):95–101.

Schousboe A. Role of astrocytes in the maintenance and modulation of glutamatergic and GABAergic neurotransmission. Neurochem Res. 2003;28(2):347–52.

Schousboe A, Waagepetersen H. Role of astrocytes in glutamate homeostasis: implications for excitotoxicity. Neurotox Res. 2005;8(3):221–5.

Schulte RF, Boesiger P. ProFit: two-dimensional prior-knowledge fitting of J-resolved spectra. NMR Biomed. 2006;19(2):255–63.

Schulte RF, Lange T, Beck J, Meier D, Boesiger P. Improved two-dimensional J-resolved spectroscopy. NMR Biomed. 2006;19(2):264–70.

Sibson NR, Dhankhar A, Mason GF, Rothman DL, Behar KL, Shulman RG. Stoichiometric coupling of brain glucose metabolism and glutamatergic neuronal activity. Proc Natl Acad Sci U S A. 1998;95(1):316–21.

Terpstra M, Ugurbil K, Gruetter R. Direct in vivo measurement of human cerebral GABA concentration using MEGA-editing at 7 Tesla. Magn Reson Med. 2002;47(5):1009–12.

Thomas MA, Yue K, Binesh N, Davanzo P, Kumar A, Siegel B, et al. Localized two-dimensional shift correlated MR spectroscopy of human brain. Magn Reson Med. 2001;46(1):58–67.

Urenjak J, Williams SR, Gadian DG, Noble M. Specific expression of N-acetylaspartate in neurons, oligodendrocyte-type-2 astrocyte progenitors, and immature oligodendrocytes in vitro. J Neurochem. 1992;59(1):55–61.

Vanhamme L, van den Boogaart A, Van Huffel S. Improved method for accurate and efficient quantification of MRS data with use of prior knowledge. J Magn Reson. 1997;129(1):35–43.

Waddell KW, Avison MJ, Joers JM, Gore JC. A practical guide to robust detection of GABA in human brain by J-difference spectroscopy at 3 T using a standard volume coil. Magn Reson Imaging. 2007;25(7):1032–8.

Wilson M, Reynolds G, Kauppinen RA, Arvanitis TN, Peet AC. A constrained least-squares approach to the automated quantitation of in vivo 1H magnetic resonance spectroscopy data. Magn Reson Med [Internet]. 2011;65(1):1–12. https://onlinelibrary.wiley.com/doi/abs/10.1002/mrm.22579.

Zierhut ML, Ozturk-Isik E, Chen AP, Park I, Vigneron DB, Nelson SJ. 1 H spectroscopic imaging of human brain at 3 Tesla: Comparison of fast three-dimensional magnetic resonance spectroscopic imaging techniques. J Magn Reson Imaging [Internet]. 2009;30(3):473–80. https://doi.org/10.1002/jmri.21834.